Bioorganic & Medicinal Chemistry Letters 19 (2009) 4067–4069

Contents lists available at ScienceDirect

Bioorganic & Medicinal Chemistry Letters

journal homepage: www.elsevier.com/locate/bmcl

Bis-anthracenyl isoxazolyl amides have enhanced anticancer activity

Mariusz P. Gajewski [a], Howard Beall [a], Mark Schnieder [a], Sarah M. Stranahan [c], Michael D. Mosher [c,d], Kevin C. Rider [b,c], Nicholas R. Natale [a,c,*]

[a] Department of Biomedical and Pharmaceutical Sciences, The University of Montana, Missoula, MT 59812, USA
[b] Core Laboratory for Neuromolecular Production, The University of Montana, Missoula, MT 59812, USA
[c] Department of Chemistry University of Idaho, Moscow, ID 83844-2343, USA
[d] Department of Chemistry, University of Nebraska-Kearney, Kearney, NE 68849-1150, USA

ARTICLE INFO

Article history:
Received 22 April 2009
Revised 1 June 2009
Accepted 3 June 2009
Available online 13 June 2009

Keywords:
Anthracene
Antitumor
Fluorescence
Glioma
G-quadruplex DNA
Isoxazole
SNB-19

ABSTRACT

Dimeric analogs of Anthracenyl Isoxazole Amides (AIMs) (the designation AIM is in honor of the memory of Professor Albert I. Meyers) were prepared and dimer **6** exhibited the highest efficacy to date for this class of anti-tumor compounds against the human glioma Central Nervous System cell line SNB-19.

We recently reported the anticancer activity of a new series of Anthracenyl Isoxazole Amides (AIMs),[1] which exhibited significant activity in the 60 Cell Line protocol at the National Cancer Institute (NCI60).[2] Our working hypothesis is that this novel class of compounds exert their effect by stabilization of quadruplex (G4) DNA,[3] either at the telomere[4] and/or specific oncogenes (Fig. 1).[5]

Recently it has been postulated that the telomeric overhang of the human chromosomes possibly forms multiple G4 conformers,[4a,b] if this argument is correct, one classic[6] test of this hypothesis would involve the tethering of G4 binding moieties, with the expectation of enhanced biological effect.

Two methods were compared for the preparation of the AIM dimers **4**–**6**. Method A utilized our previously reported lanthanide assisted Weinreb amidation,[7] or double activation methodology.[1b] Method B is a straightforward Schotten–Baumann process (Scheme 1).

The advantage of the double activation method is its directness, and it generally proceeds in overall synthetically useful yields after isolation and purification, however, in the case of AIM **4** a 2 to 1 ratio of dimer to mono-AIM incorporation was observed, though the material balance was near quantitative after the recovery of starting material. The double activation procedure was originally developed for amide couplings which were both sterically hindered and either contained functional groups incompatible with thionyl or phosphorus halides (i.e., acridines) or could be potentially chlorinated (i.e., C-10 H anthryl).[1b,9] Our recent observation that the C-10 chloro derivative **7** *actually possessed higher anticancer activity*[1a] led us to reexamine the more conventional Schotten–Baumann route. The three step Schotten–Baumann procedure first necessitates a hydrolysis, which due to the steric hindrance of the anthryl moiety proceeded in a very sluggish manner: 60 h refluxing was required for complete conversion to the carboxylic acid. The next two steps, acid chloride and amide formations, proceed

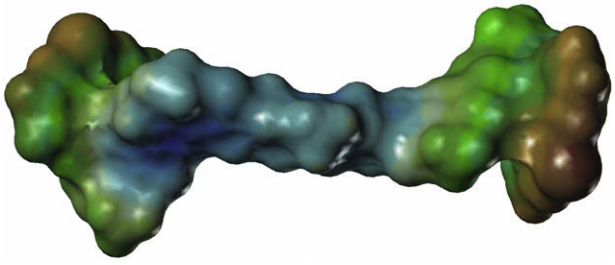

Figure 1. SYBYL (v8.0) low energy conformer of AIM dimer **6**. The MMFF94 force field and charge matrix was used, at a dielectric constant at 80. Brown: highest hydrophobic area, blue: highest hydrophilic area.

* Corresponding author. Tel.: +1 406 243 4132; fax: +1 406 243 5228.
E-mail address: nicholas.natale@umontana.edu (N.R. Natale).

0960-894X/$ - see front matter © 2009 Elsevier Ltd. All rights reserved.
doi:10.1016/j.bmcl.2009.06.019

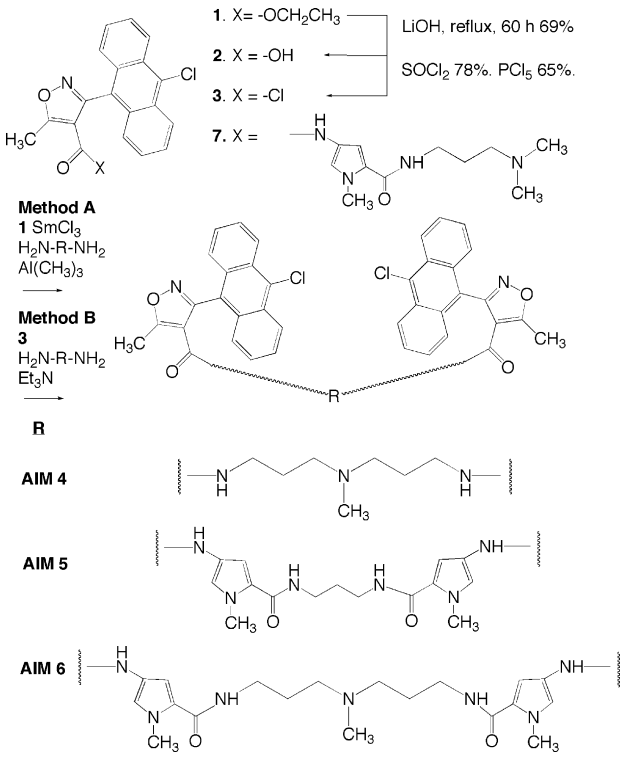

Scheme 1. Synthesis of the AIM dimers **4**–**6**.

without complication. The overall yield for the three step Schotten–Baumann process, for AIM **4,** was 24% after isolation and purification and utilizes reagents amenable to scale-up that are not pyrophoric. The overall yields from Method A and B are comparable.

There is an indication of folding of AIM **4** in solution as evidenced by magnetic anisotropy in the proton NMR.[11] No evidence for folding of the dimers containing pyrrole moieties,[8] AIMs **5** and **6**, was observed by NMR.[12,13]

The anticancer activity of the synthetic dimers assayed against a human glioma cell line, Central Nervous System (CNS) SNB-19, for AIM **4**–**7** is shown in Table 1. The effect of exposure time was examined for dimer **4**, and optimal anticancer activity was observed for 24 hour exposure time. The anticancer activities of dimers **4**–**6** were benchmarked against monomeric AIM **7**, which was among the most active of the AIM series recently reported, as measured against the NCI60, and represents the positive control.[1a] The anticancer activity of known **7** against SNB-19 cells is in good agreement with the mean graph mid-point (MG-MID) as examined in the NCI60. The AIMs which are protonated at physiological pH, **4** and **6**, were significantly more active than AIM **5**, which would be expected to be neutral. AIM **5**, while not active against SNB-19 cells, is not devoid of activity. In the NCI 60 cell line one dose study, it exhibited 66.5% tumor cell kill against the SNB-75 cell line (full NCI60 data is presented in the Supplementary data), as well as activity against non-small cell lung cancer cell HOP-92 (34.04%), ovarian cancer cells lines IGROV1 and OVCAR-4 (35.62 and 32.16%, respectively) and renal cancer cell line UO-31 (39.36%). We attribute the lower activity of **5** in our assay to its high log *P* (calculated to be ca. 7) and lack of protonation at physiological pH.

Table 1
Anticancer activity of AIM dimers **4**–**6** and control **7** against human glioma SNB-19 cells

Compd	Exposure time (h)	Cytotoxicity IC_{50}[a] (μM)	S.D.[b]
4	2	113.87	37.34
4	24	23.93	1.36
4	48	30.07	2.02
5	24	>100	na
6	24	4.75	0.27
7	24	6.21	0.21

[a] Values are means of three experiments.
[b] Standard deviation.

AIM **6** exhibited single digit micromolar inhibition of SNB-19, and at 4.75 μM represents the most efficacious analog in this class of compounds to date. Inhibition of the tumor cells lines by AIM **6** in the one dose NCI60 panel also was quite robust: a mean growth inhibition across all cell lines of 81.8% and complete inhibition of tumor cell growth was observed for 25 of the cell lines. In the five dose NCI60 the mid graph mean point for AIM **6** was −5.8, with several cells lines having nanomolar anticancer activity. Thus, the GI_{50} against Leukemia cells lines SR, MOLT-4, K-562 were 394, 615 and 822 nM, respectively.

The AIM **6** dimer, as most AIMs studied to date,[1a] exhibits useful fluorescence emission at 423 nm in ethanol solution upon excitation at 385 nm, with an approximate extinction coefficient of 20,000. The emission spectrum is shown in Figure 2. The intensity was observed to be *enhanced* both in buffer at pH 7.5 and in the presence of bovine serum albumin (BSA), and a slight wavelength shift was observed (to 430 and 431 nm, respectively). The observations are consistent with restriction of conformation movement in buffer and the presence of BSA.[10]

The pharmacokinetic properties of the AIM dimers are not ideal for potential therapeutics, in light of the fact that their high molecular weight and lipophilicity both violate Lipinski's rule of five. Lipophilicity was calculated both as *A*Log *P* using Symyx Draw, and *C*Log *D* using Chem Axon software (Supplementary data). Even for AIM **6**, which would be expected to be protonated at physiological pH, there was only a modest difference in *A*log *P* versus *C*Log *D* (7.4) of 7.0 and 6.0, respectively. However, given their robust antitumor activity and fluorescence properties, the bis-AIMs may be useful as probes and potential tools for mechanism of action studies.

In conclusion, tethering AIM moieties increases the anticancer activity of the resulting dimer, and the most active analog, AIM **6**, is—in fact—the most active AIM prepared to date. This is consistent with the hypothesis that multiple G4 conformers may be

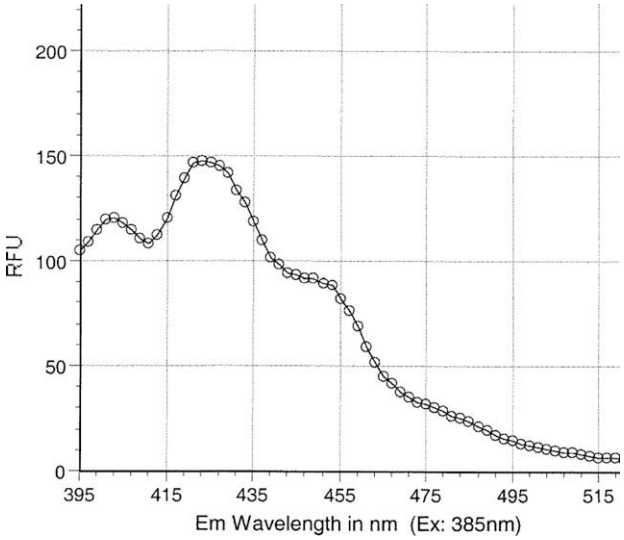

Figure 2. Fluorescence emission spectrum of AIM **6** (ethanol).

present in the telomere, and potentially represents a route to distinguish between telomeric and oncogenic G4 DNA. Future studies will be directed towards more detailed structural exploration of this unique target for anticancer drug discovery, and application of the AIMs as fluorescent probes of the mechanism of action. Our progress will be reported in due course.

Acknowledgement

The authors are grateful to the National Institutes of Health for NINDS 7R15-NS038444-04 and P20 RR015583. We thank Dr. J. B. A. (Sandy) Ross, director of the BioSpectroscopy Core at the Center for Structural and Functional Neuroscience, University of Montana, and Ayesha Sharmin for their assistance with fluorescence spectroscopy, funded by P20 RR015583. S.M.S. acknowledges summer research support from NSF REU CHE 0243760, while N.R.N. was at the University of Idaho. K.C.R. thanks P30 NS055022. We would like to thank Dr. Keith Taylor for helpful discussions on the implementation of Symyx Draw. We thank ChemAxon for use of their software. We also acknowledge Dr. David J. Burkhart of GSKBio for the use of their NMR.

Supplementary data

Supplementary data (Full experimental details for preparation of synthetic dimers **4**–**6**, procedure for Cell Culture and Growth Inhibition Assays. NSC numbers and one-dose data for **5** and **6** and five-dose data for **6** in the NCI60 protocol. Calculated log *D* graph for **6**. HSQC 2D NMR of dimer **5.** Pharmacokinetic computations for AIMs **4**–**7**) associated with this article can be found, in the online version, at doi:10.1016/j.bmcl.2009.06.019.

References and notes

1. (a) Han, X.; Li, C.; Mosher, M. D.; Rider, K. C.; Zhou, P.; Crawford, R. L.; Fusco, W.; Paszczynski, A.; Natale, N. R. *Bioorg. Med. Chem.* **2009**, *17*, 1671–1680; For a preliminary communication, see: (b) Zhou, P.; Mosher, M. D.; Taylor, W. D.; Crawford, G. A.; Natale, N. R. *Bioorg. Med. Chem. Lett.* **1997**, *7*, 2455–2456.
2. Boyd, M. R. *Princ. Pract. Oncol.* **1989**, *3*, 1–12.
3. Monchaud, D.; Teulade-Fichou, M.-P. *Org. Biomol. Chem.* **2008**, *6*, 627–636.
4. (a) De Cian, A.; Lacroix, L.; Douarre, C.; Temime-Smaali, N.; Trentesaux, C.; Riou, J.-L.; Mergny, J.-F. *Biochimie* **2008**, *90*, 131–155; (b) Xu, Y.; Noguchi, Y.; Sugiyama, H. *Bioorg. Med. Chem.* **2006**, *14*, 5584–5591; (c) Zhang, N.; Phan, A. T.; Patel, D. J. *J. Am. Chem. Soc.* **2005**, *127*, 17277–17285.
5. Siddiqui-Jain, A.; Grand, C. L.; Bearss, D. J.; Hurley, L. H. *Proc. Natl. Acad. Sci. U.S.A.* **2002**, *99*, 11593–11598.
6. Bollini, M.; Casal, J. J.; Bruno, A. M. *Bioorg. Med. Chem.* **2008**, *16*, 8003–8010.
7. (a) Basha, A.; Lipton, M.; Weinreb, S. M. *Tetrahedron Lett.* **1977**, 4171–4174; (b) Lipton, M. F.; Basha, A.; Weinreb, S. M. *Org. Synth.* **1979**, *59*, 49–53.
8. Nishiwaki, E.; Tanaka, S.; Lee, H.; Shibuya, M. *Heterocycles* **1988**, *27*, 1945–1952.
9. Han, X.; Twamley, B.; Natale, N. R. *J. Heterocycl. Chem.* **2003**, *40*, 539–545.
10. (a) Ross, J. B. A.; Laws, W. R.; Shea, M. In *Intrinsic Fluorescence in Protein Structure Analysis in Protein Structures: Methods in Protein Structure and Structure Analysis*; Unversky, V. N., Permyakov, E. A., Eds.; Nova Science: New York, 2007; (b) Sharmin, A.; Minazzo, A.; Salassa, L.; Rosenberg, E.; Ross, J. B. A.; Shariff, S. E.; Hardcastle, K. I. *Inorg. Chim Acta* **2008**, *361*, 1624–1633.
11. *3-(10-Chloro-9-anthryl)-N-[3-[3-[[3-(10-chloro-9-anthryl)-5-methylisoxazole-4-carbonyl]amino] propylmethylamino]propyl]-5-methylisoxazole-4-carboxamide, AIM 4.* ^{1}H NMR δ ppm 0.45–0.55 (m, 4H) 0.97 (t, J = 6.84 Hz, 4H) 1.20 (s, 3H) 2.62 (q, J = 6.35 Hz, 4H) 2.94 (s, 6H) 4.87 (br. s., 2H) 7.46–7.53 (m, 4H) 7.56–7.63 (m, 4H) 7.65–7.70 (m, 4H) 8.46–8.58 (m, 4H). ^{13}C NMR δ ppm 13.43; 25.89; 36.92; 40.81; 53.88; 113.14; 120.57; 125.20; 125.35; 127.33; 127.69; 128.37; 131.03; 132.35; 157.15; 160.48; 175.51. IR 3200 (NH), 2882, 1750 (C=O), 1721, cm^{-1}. Calcd for $C_{45}H_{40}N_5O_4Cl_2$ FW 783, observed FAB-MS m/z 784 [M+1^{+}, 77% Rel. I.] HR-ESMS accurate mass calcd for $C_{45}H_{40}N_5O_4Cl_2$: 784.2457, found 784.2436. 2.7 ppm.
12. *3-(10-chloro-9-anthryl)-N-[5-[3-[[4-[[3-(10-chloro-9-anthryl)-5-methylisoxazole-4-carbonyl] amino]-1-methylpyrrole-2-carbonyl] amino] propylcarbamoyl]-1-methylpyrrol-3-yl]-5-methylisoxazole-4-carboxamide, AIM 5.* TLC—R_f 0.34 (SiO_2, hexanes-ethyl acetate 6:1). ^{1}H NMR (DMSO-d_6): δ 10.18 (2H, br s), 8.53 (4H, d, J = 8.8 Hz), 7.88 (2H, d, J = 6.4 Hz), 7.75 (4H, m), 7.73 (4H, d, J = 8.8 Hz), 7.61 (4H, m), 6.86 (2H, d, J = 1.6 Hz), 6.58 (2H, d, J = 1.6 Hz), 3.61 (6H, s), 3.05 (4H, q, J = 7.2 Hz), 2.79 (6H, s), 1.27 (2H, p, J = 7.2 Hz). IR 2840, 1754, 1710 cm^{-1}. Calcd for $C_{53}H_{43}N_8O_6Cl_2$ FW 956, observed FAB-MS m/z 957 [M+1^{+}, 26.2 Rel. I.]. HR-ESMS accurate mass calcd $C_{53}H_{43}N_8O_6Cl_2$: 957.2683, found 957.2708. 2.7 ppm.
13. *3-(10-chloro-9-anthryl)-N-[5-[3-[3-[[4-[[3-(10-chloro-9-anthryl)-5-methylisoxazole-4-carbonyl]amino]-1-methylpyrrole-2-carbonyl]amino]propylmethylamino]propylcarbamoyl]-1-methylpyrrol-3-yl]-5-methylisoxazole-4-carboxamide, AIM 6.* ^{1}H NMR δ ppm 1.45–1.65 (m, 4H) 2.12 (br s., 3H) 2.29–2.45 (m, 4H) 2.96 (s, 6H) 3.09–3.28 (m, 4H) 3.59 (s, 6H) 5.30 (s, 2H) 5.67 (s, 2H) 6.27 (s, 2H) 6.53 (s, 2H) 6.77–6.91 (m, 2H) 7.40–7.51 (m, 4H) 7.56–7.65 (m, 4H) 7.66–7.76 (m, 4H) 8.53–8.67 (m, 4H). ^{13}C NMR δ ppm 13.57; 25.96; 36.31; 38.39 (br); 41.56; 56.49 (br); 102.88; 113.03; 118.00; 119.65; 120.20; 123.56; 125.28; 127.40; 127.87; 128.40; 131.10; 132.64; 157.08; 157.88; 161.10; 175.94. IR 3081, 2835, 1739 (C=O), 1716 cm^{-1}. HR-ESMS accurate mass calcd $C_{57}H_{52}N_9O_6Cl_2$: 1028.3418, found 1028.3414. 0.4 ppm.